이학석사 학위논문

Numerical Boundary Condition for the Schrödinger Equation

(슈뢰딩거 방정식의 수치적 경계 조건)

2014년 8월

서울대학교 대학원

수리과학부

권 달 현

Numerical Boundary Condition for the Schrödinger Equation

(슈뢰딩거 방정식의 수치적 경계 조건)

지도교수 강 명 주

이 논문을 이학석사 학위논문으로 제출함

2014년 4월

서울대학교 대학원

수리과학부

권 달 현

권 달 현의 이학석사 학위논문을 인준함

2014년 6월

위 원 장 ____________________ (인)

부 위 원 장 ____________________ (인)

위 원 ____________________ (인)

Numerical Boundary Condition for the Schrödinger Equation

A dissertation
submitted in partial fulfillment
of the requirements for the degree of
Master of Science
to the faculty of the Graduate School of
Seoul National University

by

Dalhyeon Gwon

Dissertation Director : Professor Myungjoo Kang

Department of Mathematical Sciences
Seoul National University

August 2014

Abstract

In this paper, we derive a high order algorithm for the 1D and 2D Schrödinger equation with Numerov method and Crank-Nicolson Scheme. In this procedure, we find discrete transparent boundary conditions for each dimensional case. Finally, we simulate this condition on a bounded interval in 1D and a bounded rectangle in 2D.

Key words: Schrödinger Equation, Transprent Boundary Condition, Numerov Method
Student Number: 2012-20241

Contents

List of Figures

Chapter 1

Introduction

The time-independent Schrödinger equation is

$$i\partial_t u = -\Delta u + V(x)u, \; x \in \mathbb{R}^n, t > 0 \tag{1.0.1}$$

$$\lim_{|x|\to\infty} u(x,t) = 0, \tag{1.0.2}$$

$$u(x,0) = u_0(x), \tag{1.0.3}$$

where V is a given real potential. We can assume that the initial function has compact support, i.e. $\mathrm{supp}(u_0) \subset B(r)$, where $B(r)$ is a ball with center at origin and radius $r > 0$. And we can assume that the potental function V is constant on $\mathbb{R}^n \setminus B(r)$ [1].

The Schrödinger equation is one of the basis equations in quantum mechanics and it appears in a number of areas of physical. Plenty of methods have been developed for the solution of the one dimentional time-independent Schrodinger equation. A well known class of the methods for the solution of the Schrödinger equation are Numerov type [8]. It is defined on the unbounded region $\Omega = \{(x,t) \in \mathbb{R}^n \times \mathbb{R}^+\}$. To restrict the computational domain, one usually imposes a boundary condition of the Dirichlet or Neumann type. For a constant exterior pontential V_{ext} in 1D, we can factorize into left and right traveling waves :

$$\begin{aligned} 0 &= \partial_x^2 u + i(\partial_t u + iV_{ext}u) && (1.0.4)\\ &= (\partial_x + e^{-i\pi/4}\sqrt[+]{\partial_t + iV_{ext}})(\partial_x - e^{-i\pi/4}\sqrt[+]{\partial_t + iV_{ext}})u && (1.0.5)\end{aligned}$$

Since the potential V is a constant function in the unbounded region, the potential may be eliminated by setting $\psi(x,t) = e^{i\mathcal{V}(t)}u(x,t)$ with $\mathcal{V}(t) = \int_0^t V(s)ds = V_{ext}t$ [2]. From (1.0.5), as a Dirichlet-Neumann map we can obtain

$$\partial_{\mathbf{n}}\psi(x,t) + e^{-i\pi/4}D_t^{1/2}\psi(x,t) = 0, \tag{1.0.6}$$

$$\text{i.e. } \partial_{\mathbf{n}}u(x,t) + e^{-i(\pi/4+V_{ext}t)}D_t^{1/2}e^{iV_{ext}t}u(x,t) = 0 \tag{1.0.7}$$

where $\mathbf{n}$ is a the outwardly directed unit normal vector to the comutational bounded domain and $D_t^{1/2}$ is the fractional derivatives with $D_t^{1/2}f(x,t) = \frac{1}{\sqrt{\pi}}\partial_t\int_0^t \frac{f(x,s)}{\sqrt{t-s}}ds$ [7].

A simple calculation shows that (1.0.7) is equivalent to the impedance boundary condition [1]

$$u(x,t) = -e^{i\pi/4}I_t^{1/2}u(x,t) = -\frac{e^{i\pi/4}}{\sqrt{\pi}}\int_0^t \frac{\partial_{\mathbf{n}}u(x,s)e^{-iV_{ext}(t-s)}}{\sqrt{t-s}}ds, \tag{1.0.8}$$

where $I_t^{1/2}f(x,t) = \frac{1}{\sqrt{\pi}}\int_0^t \frac{f(x,s)}{\sqrt{t-s}}ds$ is the fractional integral [7], in the form of a Neumann-Dirichlet map.

However, when the wave u pass trough fictive boundary, some unphysical reflections occurs. Then, one can compute on a larger computational domain which can be difficult to handle numerically and need expensive computing cost. A usual adopted solution consists in imposing a more suitable boundary condition on the fictive boundary which does not affect the solution in the interior domain by not generating any undesirable parasitic reflected waves [3].

These boundary conditions are not contained in the original problem formulation. They should be obtained by a transformation of the given asymptotic conditions at infinity onto the artificial boundary as (1.0.2) [4]. Such a transfer must provide an approximation of the solution on the unbounded domain by the solution calculated in a finite domain with an artificial boundary. Such boundary conditions are called absorbing boundary conditions if they yield a well-posed initial boundary value problem, where some energy functional is absorbed at the boundary. If this computed solution coincides on computation region with the exact solution of the whole-space problem, one refers to these boundary conditions as transparent boundary conditions [1].

In this article, we induce the high order transparent boundary condition with Numerov method on 1D and 2D in §2 and §3, respectively. And in §4, we show implementation for each dimension and analysis.

Chapter 2

Transparent Boundary Condition

2.1 Numerov Method

The Numerov method is used to solve diffential equation of the form

$$\frac{d^2u}{dx^2} = f(x,u). \tag{2.1.1}$$

The Taylor expansion of u at $x = x_0 + h$ and $x = x_0 - h$ is

$$u(x_0+h) = u(x_0)+hu'(x_0)+\frac{h}{2!}u''(x_0)+\frac{h^2}{3!}u^{(3)}(x_0)+\frac{h^4}{4!}u^{(4)}(x_0)+\frac{h^5}{5!}u^{(5)}(x_0)+O(h6),$$

$$u(x_0-h) = u(x_0)-hu'(x_0)+\frac{h}{2!}u''(x_0)-\frac{h^2}{3!}u^{(3)}(x_0)+\frac{h^4}{4!}u^{(4)}(x_0)-\frac{h^5}{5!}u^{(5)}(x_0)+O(h6).$$

We replace those expression by $u_{n-1} = u(x_0 - h), u_n = u(x_0)$ and $u_{n+1} = u(x_0 + h)$. The sum of those two equations gives

$$u_{n+1} + u_{n-1} = 2u_n + h^2u''_n + \frac{h^4}{12}u_n^{(4)} + O(h^6).$$

Since $u_n'' = f_n$ and $u_n^{(4)} = \dfrac{d^2}{dx^2} f_n = \dfrac{f_{n+1} - 2f_n + f_{n-1}}{h^2} + O(h^2)$, we can get following scheme :

$$u_{n+1} + u_{n-1} = 2u_n + h^2 f_n + \frac{h^4}{12} \frac{f_{n+1} - 2f_n + f_{n-1}}{h^2} + O(h^6),$$

$$\text{i.e. } u_{n+1} = 2u_n - u_{n-1} + h^2 \frac{f_{n+1} + 10f_n + f_{n-1}}{12} + O(h^6). \tag{2.1.2}$$

(2.1.2) is called the Numerov method for nonlinear equations of fourth order. It is implicit, but can be made explicit if the equation is linear.

2.2 Transparent Boundary Condition in One Dimension

The original transparent boundary condition formulation for the Schrödinger equation dates to 1982, but recently has the proper discretization of the results been given [9]. With discrete transparent boundary conditions, there is no need to artificially impose restrictions on space and time.

At (1.0.1), we define the Hamiltonian operator $H = -\dfrac{\partial^2}{\partial x^2} + V(x)$ and the system propagator $exp(-iHt)$. Then (1.0.1) is written as following with initial wave function $\psi(x, t_0)$:

$$\psi(x, t + \Delta) = exp(-iH\Delta)\psi(x, t). \tag{2.2.1}$$

$exp(-iH\Delta)$ is approximated with the Cayley form,

$$exp(i - H\Delta) = \frac{1 - iH\Delta/2}{1 - iH\Delta/2} + O(\Delta^2). \tag{2.2.2}$$

Combining (2.2.1) and (2.2.2), we can obtain the Crank-Nicholson approximation to the evolution problem,

$$\left[1 + i\frac{H\Delta}{2}\right] \psi(x, t + \Delta) \approx \left[1 - i\frac{H\Delta}{2}\right] \psi(x, t). \tag{2.2.3}$$

We rewrite (2.2.3) with new function $y(x, t) \equiv \psi(x, t+\Delta) + \psi(x, t)$ and using the definition of H,

$$\frac{\partial^2 y}{\partial x^2} - \left[V(x) - i\frac{2}{\Delta}\right] y(x, t) = i\frac{4}{\Delta}\psi(x, t). \tag{2.2.4}$$

2.2.1 Numerov Approximation

Equation (2.2.4) has of the form $y''(x) = g(x)y(x) + f(x,t)$ with $g(x) = V(x) - \frac{2i}{\Delta}$ and $f(x,t) = 4i\frac{\psi(x,t)}{\Delta}$. We usually use the central-space scheme to approximate the second derivative. We abbreviate $y_j^n = y(x_0 + j\Delta_x, t_0 + n\Delta_t)$ $g_j = g(x_0 + j\Delta_x)$, and similarly for the others. Now, we use the numerov method to obtain high order scheme. From Sec. 2.1 procedure,

$$\begin{aligned} y_{j+1}^n - 2y_j^n + y_{j-1}^n &= h^2\left(g_j y_j^n + f_j^n\right) \\ &+\frac{h^2}{12}\left(g_{j+1}y_{j+1}^n + f_{j+1}^n - 2g_j y_j^n - 2f_j^n + g_{j-1}y_{j-1}^n + f_{j-1}^n\right), \end{aligned}$$

$$\text{i.e. } w_{j+1}^n + w_{j-1}^n = \left[2 + h^2\frac{g_j}{d_j}\right] w_j^n + h^2\frac{f_j^n}{d_j}, \tag{2.2.5}$$

where $d_j \equiv 1 - h^2\frac{g_j}{12}$ and $w_j^n \equiv d_j y_j^n - h^2\frac{f_j^n}{12}$. In terms of the new functions, the result takes the very simple form.

Since equation (2.2.5) has recursion relation for the w_j^n, the numerical solution is obtained if we have initial value w_0^n and w_0^n. We want to reduce the three-term recursions relation (2.2.5) to the two-term recursions of the form $w_{j+1}^n = e_j w_j^n + q_j^n$. From (2.2.5), we obtain

$$e_j + \frac{1}{e_{j-1}} = 2 + h^2\frac{g_j}{d_j} \tag{2.2.6}$$

$$q_j^n = \frac{q_{j-1}^n}{e_{j-1}} + h^2\frac{f_j^n}{d_j}. \tag{2.2.7}$$

Equation (2.2.6) and (2.2.7) generate e_j and g_j^n for $j = 1, \cdots, J-1$ from the initial e_0 and q_0^n. We can assume vanishing w_j^n at the boundary, i.e. $w_0^n = w_J^n = 0$. The two-for-one replacement means that one of these data points may be chosen arbitrarily, while the other is dictated by the boundary conditions. The trick is to recognize that for rigid walls ($w_J^n = 0$), we can let $e_0 \to \infty$, thus permitting both e_j and q_j^n to be found immediately from (2.2.6) and (2.2.7), assuming only that q_0^n is finite. We can note that the e_j only depend on the position variable, i.e. e_j be computed just once at the start of the process. On the other hand, q_j^n has the position and time variable, must be computed at each time step. Starting with $w_J^n = 0$, we use relation $w_{j-1}^n = \dfrac{w_j^n - q_{j-1}^n}{e_{j-1}}$ to calculate w_{J-1}, w_{J-2}, $\cdots$, w_1^n.

In any case, the rigid-wall boundary conditions unacceptable limitations in scattering problems or other sitiations where the wave function is not inherently confined. With discrete transparent boundary conditions, these limitations can be overcome [9].

2.2.2 Transparent Boundary Conditions

We now derive the discrete transparent boundary conditions using the Numerov approximation with the Crank-Nicholson evolution problem. Computed interval must support the initial wave function, which is required to vanish in the exterior. Our derivation start with equation (2.2.5). (2.2.5) will be solved exactly in the exterior regions to obtain the proper connections at $j = 0$ and $j = J$.

Several transforms are used solving partial differential equation to reduce computed variable. (2.2.5) has two difference relation in both the space and time indices. To remove time index, we consider the $\mathcal{Z}$-transform defined by

$$\widetilde{\psi}_i(z) = \sum_{n=0}^{\infty} \psi_j^n z^{-n}.$$

This is the discrete analogue of the Laplace transform defined by

$$\widetilde{f}(s) = \int_0^{\infty} f(t) e^{-st} dt,$$

for the complex number s. $\mathcal{Z}$-transform can be applied to the solution of linear difference equations in order to reduce the solutions of such equations into those of algebraic equations in the complex plain.

Assume that the exterior region is force-free, i.e. $V \equiv 0$, so that g_j and d_j become constants, denoted by g and d. By $\mathcal{Z}$-transform, (2.2.5) becomes

$$\left[d(z+1) - i\frac{h^2}{3\Delta}\right]\left[\widetilde{\psi}_{j+1}(z) + \widetilde{\psi}_{j-1}(z)\right] = 2a\left[d(z+1) - i\frac{h^2}{3\Delta}\right]\widetilde{\psi}_j(z) + i\frac{4h}{d\Delta}\widetilde{\psi}_j(z)$$

or,

$$\widetilde{\psi}_{j+1}(z) + \widetilde{\psi}_{j-1}(z) = 2a\widetilde{\psi}_j(z) + i\frac{2\lambda}{d^2}\frac{1}{z+c}\widetilde{\psi}_j(z), \tag{2.2.8}$$

where constants $a = 1 + \dfrac{h^2 g}{2d}$, $\lambda = \dfrac{2h^2}{\Delta}$ and $c = 1 - \dfrac{2\lambda}{6d}$. We try a previous method of solution, that is, introduce auxiliary functions $e_j(z)$ and $q_j(z)$ such that

$$\widetilde{\psi}_{j+1}(z) = e_j(z)\widetilde{\psi}_j(z) + q_j(z). \tag{2.2.9}$$

Combining (2.2.8) and (2.2.9), we see that

$$e_j(z) + \frac{1}{e_{j-1}(z)} = 2a + i\frac{2\lambda}{d^2}\frac{1}{z+c} \tag{2.2.10}$$

$$q_j(z) = \frac{q_{j-1}(z)}{e_{j-1}(z)}. \tag{2.2.11}$$

Since (2.2.10) has no j on the right hand side, the recoursion relation for $e_j(z)$ is satisfied by a uniform $e_j(z) = e(z)$. (2.2.10) reduces to a quadratic equation for $e(z)$,

$$e^2(z) - \left(2a + i\frac{2\lambda}{d^2}\frac{1}{z+c}\right)e(z) + 1 = 0. \tag{2.2.12}$$

Two roots $e_\pm(z)$ satisfy $e_+(z)e_-(z) = 1$. On the left of the computed region, $j = 0, -1, \cdots$, we choose the root $|e(z)| > 1$. From (2.2.11),

$$q_j(z) = \frac{q_{j-1}(z)}{e(z)} = \frac{q_{j-2}(z)}{e^2(z)} = \cdots == \frac{q_{j-N}(z)}{e^N(z)} \to 0.$$

Similarly, on the right of the computed region, we take the root $|e(z)| < 1$. Then,

$$q_j(z) = e(z)q_{j+1}(z) = e^2(z)q_{j+2}(z) = \cdots = e^N(z)q_{j+N}(z) \to 0.$$

In this way, problem in both exterior region is reduced to

$$\widetilde{\psi}_{j+1}(z) = e_j(z)\widetilde{\psi}_j(z), \tag{2.2.13}$$

with proper $e(z)$. Using (2.2.13), we obtain $\widetilde{\psi}_j$ for the exterior region. But, inverse $\mathcal{Z}$-transform requires enormous computational cost. Fortunately, we need to compute only the boundary conditions, i.e. at $j = 0, J$.

From equation (2.2.12), the roots $e_{\pm}(z)$ is written an following explicit form :

$$e_{\pm}(z) = \frac{az + a'c \pm z\sqrt{a^2-1}\sqrt{1-2\mu x + x^2}}{z+c}$$

with $\mu = \dfrac{1-|a|^2}{|1-a^2|}$, $x = \dfrac{e^{-i\phi}}{z}$, $\phi = arg\left(\dfrac{a^2-1}{c}\right)$. Since inverse $\mathcal{Z}$-transform requires a representation of invese power of z, we need to recalculate square root terms. Note that $\dfrac{1}{\sqrt{1-2\mu x + x^2}} = P_n(\mu)x^n$, where $P_n(\mu)$ is an nth degree Legendre polynomial. With a tedious computing, we find

$$\sqrt{1-2\mu x + x^2} = -\sum_{n=0}^{\infty} l_n z^{-n},$$

$$l_n = \frac{e^{-in\phi}}{2n-1}\left(P_n(\mu) - P_{n-2}(\mu)\right),\ l_0 = -1, \text{and } l_1 = \mu e^{-i\phi}.$$

With this result, equation (2.2.13) at $j = 0$ becomes

$$(z+c)\widetilde{\psi}_1(z) = \left(az + a'c \mp z\sqrt{a^2-1}\sum_{n=0}^{\infty} l_n z^{-n}\right)\widetilde{\psi}_0(z).$$

Through inverse $\mathcal{Z}$-transform, we obtain the transparent boundary condition on the left

$$\psi_1^{n+1} + c\psi_1^n = (a \pm \sqrt{a^2-1})\psi_0^{n+1} + a'c\psi_0^n \mp \sqrt{a^2-1}\sum_{k=1}^{n} l_{n-k+1}\psi_0^k$$

or,

$$w_1^n = (a \pm \sqrt{a^2-1})w_0^n + \left(a' - a \mp \sqrt{a^2-1}\right)d'\psi_0^n \mp d\sqrt{a^2-1}\sum_{k=1}^{n} l_{n-k+1}\psi_0^k. \tag{2.2.14}$$

Similarly, we obtain the transparent boundary condition on the right

$$\psi_{J-1}^{n+1} + c\psi_{J-1}^n = (a \mp \sqrt{a^2-1})\psi_J^{n+1} + a'c\psi_J^n \pm \sqrt{a^2-1}\sum_{k=1}^{n} l_{n-k+1}\psi_J^k$$

or,

$$w_{J-1}^n = (a \mp \sqrt{a^2-1})w_J^n + \left(a' - a \pm \sqrt{a^2-1}\right) d'\psi_J^n \pm d\sqrt{a^2-1}\sum_{k=1}^{n} l_{n-k+1}\psi_J^k. \tag{2.2.15}$$

In §2.2.1, we make the two-term recursions of the form $w_{j+1}^n = e_j w_j^n + q_j^n$. Compared with equation (2.2.14), we find the following :

$$\begin{aligned} w_1^n &= e_0 w_0^n + q_0^n && (2.2.16)\\ e_0 &= a_0 \pm \sqrt{a_0^2-1}, && (2.2.17)\\ q_0^n &= d_0'(a_0' - e_0)\psi_0^n + d_0(a_0 - e_0)\sum_{k=1}^{\infty} l_{n-k+1}\psi_0^k, && (2.2.18) \end{aligned}$$

where $d_0 = 1 - \dfrac{h^2 g_0}{12}$ and $a_0 = 1 + \dfrac{h^2 g_0}{12 d_0}$. The sign in (2.2.17) is decided by the requirement that $|e_0| > 1$. Notice that to compute q_0^n, we need, in addition to the current value of ψ, all earlier values ψ_0^k which occur in the convolution on the right side of equation (2.2.18) [9]. Since initial value e_0 and q_0 is given by equation (2.2.17) and (2.2.18), we can find the remaining e_j and q_j using (2.2.6) and (2.2.7).

Like this procedure, we can write boundary condition on the right as :

$$\begin{aligned} w_{J-1}^n &= \alpha_J w_J^n + \beta_J^n && (2.2.19)\\ \alpha_J &= a_J \pm \sqrt{a_J^2-1}, && (2.2.20)\\ \beta_J^n &= d_J'(a_J' - \alpha_J)\psi_J^n + d_J(a_J - \alpha_J)\sum_{k=1}^{\infty} l_{n-k+1}\psi_J^k. && (2.2.21) \end{aligned}$$

Also, the sign in (2.2.20) is selected by $|\alpha_J| > 1$. Since we have relation $w_J^n = e_{J-1}w_{J-1}^n + q_{J-1}^n$, we find the intial value for w_J^n,

$$w_J = \frac{q_{J-1}^n + \beta_J^n e_{J-1}}{1 - \alpha_J e_{J-1}}. \tag{2.2.22}$$

And then, using $w_{j-1}^n = \dfrac{w_j^n - q_{n-1}^n}{e_{j-1}}$, we generate $w_{J-1},\ w_{J-2}, \cdots,\ w_0^n$ in inverse sequence. Our purpose is computing wave function ψ_j^n which is recovered from w_j^n :

$$\psi_j^{n+1} = -\psi_j^n + i\frac{h^2}{3\Delta d_j}\psi_j^n + \frac{w_j^n}{d_j}. \tag{2.2.23}$$

2.3 Transparent Boundary Condition in Two dimension

The original form of the Schrödinger equation is

$$i\hbar\frac{\partial}{\partial t}\psi(x,t) = -\frac{\hbar}{2m}\Delta\psi(x,t) + V(x,t)\psi(x,t),\ x \in \mathbb{R}^n,$$

where $m \approx 0.568544\times10^{-11}eV/C^2$ is the particle's mass and $\hbar \approx 1.054571726\times 10^{-34}Js$ is the Planck constant which describes the relationship between energy and frequency. However, these are extremely small used in computing science. Through the change of variable, we can set m and $\hbar$ any constant, e.g. $m = \dfrac{1}{2}$ and $\hbar = 1$ in (1.0.1). In this section, we start with putting $m = 1$ and $\hbar = 1$, i.e.

$$i\partial_t\psi(x,y,t) = -\frac{1}{2}\Delta\psi(x,y,t) + V(x,y,t)\psi(x,y,t),\ (x,y) \in \mathbb{R}^2. \tag{2.3.1}$$

2.3.1 Numerov Approximation

As previous §2.2, Numerov method will be used with a Crank-Nicolson scheme in time, which yields an unconditionally stable scheme [11]. We know the standard finite difference operators :

$$\begin{aligned}
D_t^+\psi_{j,k}^n &= \frac{\psi_{j,k}^{n+1} - \psi_{j,k}^n}{\Delta t}, \\
D_x^2\psi_{j,k}^n &= \frac{\psi_{j+1,k}^n - 2\psi_{j,k}^n + \psi_{j-1,k}^n}{\Delta^2}, \\
D_y^2\psi_{j,k}^n &= \frac{\psi_{j,k+1}^n - 2\psi_{j,k}^n + \psi_{j,k-1}^n}{\Delta^2}.
\end{aligned}$$

And we abbreviate

$$\begin{aligned} \psi_{j,k}^{n+\frac{1}{2}} &= \frac{1}{2}\left(\psi_{j,k}^{n+1} + \psi_{j,k}^{n}\right), \\ V_{j,k}^{n+\frac{1}{2}} &= V\left(x_j, y_k, t_{n+\frac{1}{2}}\right). \end{aligned}$$

With the discretization in time and the Crank-Nicolson scheme, (2.3.1) becomes

$$\Delta\psi^{n+\frac{1}{2}} = 2V^{n+\frac{1}{2}}(x,y)\psi^{n+\frac{1}{2}}(x,y) - 2iD_t^+\psi^n(x,y). \tag{2.3.2}$$

Using nine-point scheme, we derive second order difference operator

$$D^2 = D_x^2 + D_y^2 + \frac{\Delta x^2 + \Delta y^2}{12} D_x^2 D_y^2.$$

With the identity operator I, we generalize the 1D case in §2.2.1 :

$$D^2\psi_{j,k}^{n+\frac{1}{2}} = \left(I + \frac{\Delta x^2}{12}D_x^2 + \frac{\Delta y^2}{12}D_y^2\right)\left[2V_{j,k}^{n+\frac{1}{2}}\psi_{j,k}^{n+\frac{1}{2}} - 2iD_t^+\psi_{j,k}^n\right]. \tag{2.3.3}$$

Consider the Schrödinger equation

$$\begin{aligned} i\partial_t\psi(x,y,t) &= -\frac{1}{2}\Delta\psi(x,y,t) + V(x,y,t)\psi(x,y,t),\ (x,y) \in \mathbb{R}^2 && (2.3.4) \\ \psi(x,y,0) &= \psi_0(x,y) && (2.3.5) \\ \psi(x,0,t) &= \psi(x,Y,t) = 0. && (2.3.6) \end{aligned}$$

on the infinite stripe $\Omega = \mathbb{R} \times (0,Y)$. We will compute on bounded region $(0,X) \times (0,Y) \supset supp\,(\psi_0(x,y))$. We assume the potential $V(x,y,t)$ is constant on each of the two exterior region. The discretization of (2.2.4) with (2.2.3) is

$$\begin{aligned} &(1-\alpha_{j+1,k}^n)\psi_{j+1,k}^{n+1} + (1-\alpha_{j-1,k}^n)\psi_{j-1,k}^{n+1} + (D-\alpha_{j,k+1}^n)\psi_{j,k+1}^{n+1} + (1-\alpha_{j,k-1}^n)\psi_{j,k-1}^{n+1} \\ &\quad +\beta_{j,k}^n\psi_{j,k}^{n+1} + C\left(\psi_{j+1,k+1}^{n+1} + \psi_{j+1,k-1}^{n+1} + \psi_{j-1,k+1}^{n+1} + \psi_{j-1,k-1}^{n+1}\right) \\ &= (2W-1+\alpha_{j+1,k}^n)\psi_{j+1,k}^n + (2W-1+\alpha_{j-1,k}^n)\psi_{j-1,k}^n \\ &\quad +(2W-D+\alpha_{j,k+1}^n)\psi_{j,k+1}^n + (2W-D+\alpha_{j,k-1}^n)\psi_{j,k-1}^n + (16W-\beta_{j,k}^n)\psi_{j,k}^n \\ &\quad -C\left(\psi_{j+1,k+1}^n + \psi_{j+1,k-1}^n + \psi_{j-1,k+1}^n + \psi_{j-1,k-1}^n\right) \end{aligned}$$

(2.3.7)

with the abbreviations

$$D = \frac{\Delta x^2}{\Delta y^2},\ C = \frac{\Delta x^2 + \Delta y^2}{12\Delta y^2},\ W = \frac{i\Delta x^2}{12\Delta t},$$
$$\alpha^n_{j,k} = 2C - W + \frac{\Delta x^2}{6} V^{n+\frac{1}{2}}_{j,k},\ \beta^n_{j,k} = -2 - 2D - 8\alpha^n_{j,k} + 20C.$$

2.3.2 Transparent Boundary Condition

Transparent boundary condition is derived on the exterior region and matched at boundary with the interior computed region. Define the discrete sine-transform in y-direction on Ω^C

$$\widehat{\psi}^{n+1}_{j+1,m} = \frac{2}{K}\sum_{k=1}^{K-1} \psi^n_{j,k} \sin\left(\frac{\pi k m}{K}\right),\ m = 1,\ 2, \cdots,\ K-1$$

for $j \leq 0$and $j \geq J$. By sine-tranform, Relation (2.3.7) becomes

$$\begin{aligned}&\gamma_m \widehat{\psi}^{n+1}_{j+1,m} + \rho_m \widehat{\psi}^{n+1}_{j,m} + \gamma_m \widehat{\psi}^{n+1}_{j-1,m} \\ &\quad = (2W - \gamma_m)\,\widehat{\psi}^n_{j+1,m} + (\kappa_m - \rho_m)\,\widehat{\psi}^n_{j,m} + (2W - \gamma_m)\,\widehat{\psi}^n_{j-1,m} \qquad (2.3.8)\end{aligned}$$

with the abbreviations

$$\begin{aligned}\gamma_m &= 1 + 2C\left(\cos\left(\frac{\pi m}{K}\right) - 1\right) + W - \frac{\Delta x^2}{6}V, \\ \kappa_m &= 4\left(\cos\left(\frac{\pi m}{K}\right) + 4\right)W, \\ \rho_m &= -2 - 2D + 4C + 8W - \frac{4\Delta x^2}{3}V \\ &\quad + \left(2D - 4C + 2W - \frac{\Delta x^2}{3}\right)\cos\left(\frac{\pi m}{K}\right).\end{aligned}$$

Since the potential V is a constant function on Ω^C, it doesn't need any indices. Relation (2.3.8) is worthy of notice. For each $m = 1, \cdots, K-1$, it seems like 1-dimensional 3-points scheme. Therefore we can guess obtaining transparent boundary conditions as §2.2.

(2.3.8) has a different times data, and we are using $\mathcal{Z}$-transform

$$\Psi_{j,m}(z) = \sum_{n=0}^{\infty} \widehat{\psi}_{j,m}^{n} z^{-n}.$$

We assume the initial function $\psi_{j,k}^0 = 0$ at $j \leq 1$ and $j \geq J-1$ for all k. The $\mathcal{Z}$-transform of (2.3.8) is

$$\Psi_{j+1,m}(z) + \left[\frac{\rho_m(z+1) - \kappa_m}{\gamma_m(z+1) - 2W}\right] \Psi_{j,m}(z) + \Psi_{j-1,m}(z) = 0 \tag{2.3.9}$$

for $j \geq J$, $m = 1, \cdots, K-1$. (2.3.9) is a second order recurrence relation, or a second order finite difference equation. Its characteristic equation has two solutions $\nu_m^{(1)}(z), \nu_m^{(2)}(z)$ with $\nu_m^{(1)}(z) \cdot \nu_m^{(2)}(z) = 1$. Explicitly,

$$\nu_m^{\pm}(z) = \frac{-\rho_m(z+1) + \kappa_m \pm \sqrt{\zeta_m z^2 - 2\xi_m z + \theta_m}}{2\gamma_m(z - \eta_m)}.$$

with

$$\begin{aligned}
\eta_{J,m} &= (\rho_{J,m})^2 - 4(\gamma_{J,m})^2, \\
\theta_{J,m} &= (\kappa_m - \rho_{J,m})^2 - 4(\gamma_{J,m}\eta_{J,m})^2 \\
\xi_{J,m} &= -(\rho_{J,m})^2 - 4(gamma_{J,m})^2\eta_{J,m} + \rho_{J,m}\kappa_m.
\end{aligned}$$

For each $m = 1, \cdots, K-1$, we choose the solution such that $|\nu_m(z)| < 1$. The corresponding, decaying solution $\Psi_{j,m}(z) = (\nu_m(z))^j$, $j \geq J$ of (2.3.9) then yeilds the $\mathcal{Z}$-transformed transparent boundary conditions at $j = J$:

$$\Psi_{J,m}(z) = \nu_m(z)\Psi_{j-1,m}(z).$$

for $m = 1, \cdots, K-1$. Similarly, we can get a condition at $j = 0$. For $j = 0, J$ and $m = 1, \cdots, K-1$, $\nu_m(z)$ becomes

$$\begin{aligned}
\mathcal{Z}^{-1}(\nu_{j,m}(z))^{(n)} &= l_{j,m}^{(n)} \\
&= -\frac{\rho_{j,m}}{2\gamma_{j,m}}\eta_{j,m}^{n} + \frac{\kappa_m - \rho_{j,m}}{2\gamma_{j,m}}\left(\eta_{j,m}^{n-1} - \frac{\delta_n^0}{\eta_{j,m}}\right) \\
&\quad + \frac{\sqrt{\theta_{j,m}}}{2\gamma_{j,m}}\lambda_{j,m}^{1-n}\left[P_n(\mu_{j,m}) - \frac{P_{n-1}(\mu_{j,k})}{\eta_{j,m}\lambda_{j,m}}\right] \\
&\quad + \frac{\sqrt{\theta_{j,m}}}{2\gamma_{j,m}}\lambda_{j,m}^{1-n}\frac{\tau_{j,m}}{\zeta_{j,m}\eta_{j,m}}\sum_{k=0}^{n-1}(\lambda_{j,m}\eta_{j,m})^{n-k}P_k(\mu_{j,m})
\end{aligned}$$

(2.3.10)

with the Legendre polynomials P_n, the Kronecker symbol δ_n^0, $\lambda_{j,m} = \dfrac{\sqrt{\zeta_{j,m}}}{\sqrt{\theta_{j,m}}}$, $\nu_{j,m} = \dfrac{\xi_{j,m}}{\sqrt{\theta_{j,m}}\sqrt{\zeta_{j,m}}}$, and $\tau_{j,m} = \dfrac{\theta_{j,m}}{\eta_{j,m}} + \zeta_{j,m}\eta_{j,m} - 2\xi_{j,m}$ by the inverse $\mathcal{Z}$-transform.

By this results, the sine-transformed discrete transparent boundary conditions at $j = 0$ and $j = J$ for the discretization scheme (2.3.7) is given as following :

$$\begin{aligned} \widehat{\psi}^n_{1,m} - l^{(0)}_{0,m}\widehat{\psi}^n_{0,m} &= \sum_{k=1}^{n-1} l^{(n-k)}_{0,m}\widehat{\psi}^k_{0,m} && (2.3.11)\\ \widehat{\psi}^n_{J-1,m} - l^{(0)}_{J,m}\widehat{\psi}^n_{J,m} &= \sum_{k=1}^{n-1} l^{(n-k)}_{J,m}\widehat{\psi}^k_{J,m}. && (2.3.12) \end{aligned}$$

Since (2.3.10) and (2.3.11) are local in the y-Fourier space, this is the efficient way to implement them.

The convolution coefficients $l^{(n)}_{0,m}$ are asymptotically an oscillatory sequence. Moreover, this behavior deviates from the $O(t^{-\frac{3}{2}})$-decay of the continuous convolution kernel in (1.0.6). Hence, it may lead to numerical cancellations in the calculation of the convolution sums (2.3.11), (2.3.12) [10]. It is related with classical result on the asymptotic property of the Legendre polynomials [6]:

$$P_n(\cos\theta) = \frac{\sqrt{2}}{\sqrt{\pi}\sqrt{\sin\theta}} \frac{\cos\left(\left(n+\frac{1}{2}\right)\theta - \frac{\pi}{4}\right)}{\sqrt{n}} + O(n^{-\frac{3}{2}}),\ 0 < \theta < \pi.$$

As an alternative, we derive coefficients that decay like $O(t^{-\frac{3}{2}})$. For the left DTBCs, we add equation (2.3.11) for n and $n-1$ with the corresponding weighting factors 1 and $-\eta_{1,m}$, and so is (2.3.12) $j = J$ [10]. Therefore DTBC is given the following

$$\widehat{\psi}^n_{1,m} - s^{(0)}_{0,m}\widehat{\psi}^n_{0,m} = \sum_{k=1}^{n-1} s^{(n-k)}_{0,m}\widehat{\psi}^k_{0,m} + \eta_{1,m}\widehat{\psi}^{n-1}_{1,m} \tag{2.3.13}$$

$$\widehat{\psi}^n_{J-1,m} - s^{(0)}_{J,m}\widehat{\psi}^n_{J,m} = \sum_{k=1}^{n-1} s^{(n-k)}_{J,m}\widehat{\psi}^k_{J,m} + \eta_{J,m}\widehat{\psi}^{n-1}_{J,m}. \tag{2.3.14}$$

for $n \geq 1$ with the summed coefficients

$$s^{(n)}_{j,m} = \begin{cases} l^{(n)}_{j,m} - \eta_{j,m} l^{(n-1)}_{j,m}, & n \geq 1 \\ l^{(0)}_{j,m}, & n = 0 \end{cases}$$

for $m = 1, \cdots, K-1$, $j = 0$ and $j = J$. For $n \geq 2$,

$$\begin{aligned} s^{(n)}_{j,m} &= \frac{\sqrt{\theta_{j,m}}}{2\gamma_{j,m}}\lambda^{1-n}_{j,m}\Bigg[P_n(\mu_{j,m}) + P_{n-2}(\mu_{j,m}) - \frac{1}{\eta_{j,m}\lambda_{j,m}}P_{n-1}(\mu_{j,m}) \\ &\quad -\eta_{j,m}\lambda_{j,m}P_{n-1}(\mu_{j,m}) + \frac{\tau_{j,m}\lambda_{j,m}}{\zeta_{j,m}}P_{n-1}(\mu_{j,m})\Bigg]. \end{aligned}$$

Since the recurrence relation for the Legendre polynomials

$$nP_n(\mu_{j,m}) = (2n-1)\mu_{j,m}P_{n-1}(\mu_{j,m}) - (n-1)P_{n-2}(\mu_{j,m}),$$

for $n \geq 2$ then follows

$$s^{(n)}_{j,m} = -\frac{\sqrt{\theta_{j,m}}}{2\gamma_{j,m}}\lambda^{1-n}_{j,m}\frac{P_n(\mu_{j,m}) - P_{n-2}(\mu_{j,m})}{2n-1}. \tag{2.3.15}$$

(2.3.13) and (2.3.14) are non-local in time. It is necessary to compute a convolution of size n in the n-th step. It occurs a quadratic growing numerical cost. In [6] and [10], the authors derived an approximation of the convolution coefficients by a sum of exponentials. If one want to reduce computation cost, it is a good alternative plan.

Chapter 3

Implementation

3.1 1D Schrödinger Equation

Most simple case of a quantum wave function is the free Gaussian wave packet. Define wave function as

$$\psi(x) = \frac{1}{(2\pi\sigma^2)^{-1/4}} \exp\left(-\frac{(x-x_0)^2}{2\sigma^2}\right)$$

where $\sigma = 0.125$ and $x_0 = 0.5$. The computation domain is a unit interval $[0,1]$ with $\Delta x = \frac{1}{1600}$, $\Delta t = 10^{-3}$. Fig 3.1 shows the $|\psi(x,t)|$ at time $t = 0,\ 10\Delta t,\ 20\Delta t$, and $30\Delta t$. As our guess, there is no reflection at the both boundary and wave spreads uniformly.

Second case is a free particle with nonzero velocity. Let's define wave function as follow :

$$\psi(x) = \frac{1}{(2\pi\sigma^2)^{-1/4}} \exp(ikx) \exp\left(-\frac{(x-x_0)^2}{2\sigma^2}\right)$$

with $k = 50$, $\sigma = 0.125$ and $x_0 = 0.2$.. Fig 3.2 shows the results with $\Delta x = \frac{1}{1600}$, $\Delta t = 2 \cdot 10^{-3}$ at time $t = 0,\ 10\Delta t,\ 20\Delta t$, and $30\Delta t$. This

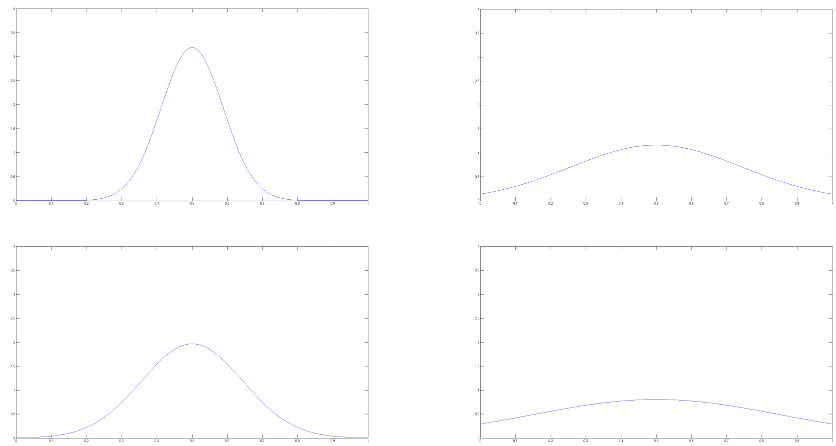

Figure 3.1: Free particle with $k = 0$(no velocity), $\sigma = 0.125$, $x_0 = 0.5$, $\Delta x = \dfrac{1}{1600}$, $\Delta t = 10^{-3}$ at time $t = 0,\ 10\Delta t,\ 20\Delta t$, and $30\Delta t$.

particle travels to the right and spreads uniformly. And there is no reflection on the right boundary.

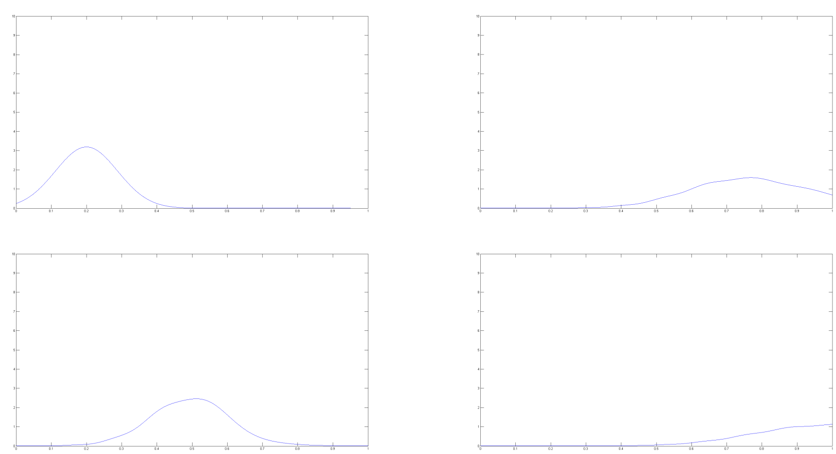

Figure 3.2: Free particle with velocity $k = 50$, $\sigma = 0.125$, $x_0 = 0.5$, $\Delta x = \dfrac{1}{1600}$, $\Delta t = 10^{-3}$ at time $t = 0,\ 10\Delta t,\ 20\Delta t$, and $30\Delta t$.

Third case contains the nonzero potential function. The potential is given as $V(x) = 2 \cdot 10^3$ on $[0.8, 0.82]$. Initial wave function is given as second case. As expected, no reflection at both boundary. We can observe quantum tunneling, a particle tunnels through a barrier that it classically could not surmount. Tunnelling is often explained using the Heisenberg uncertainty principle and the wave–particle duality of matter. Pure quantum mechanical concepts are central to the phenomenon, so quantum tunnelling is one of the novel implications of quantum mechanics.

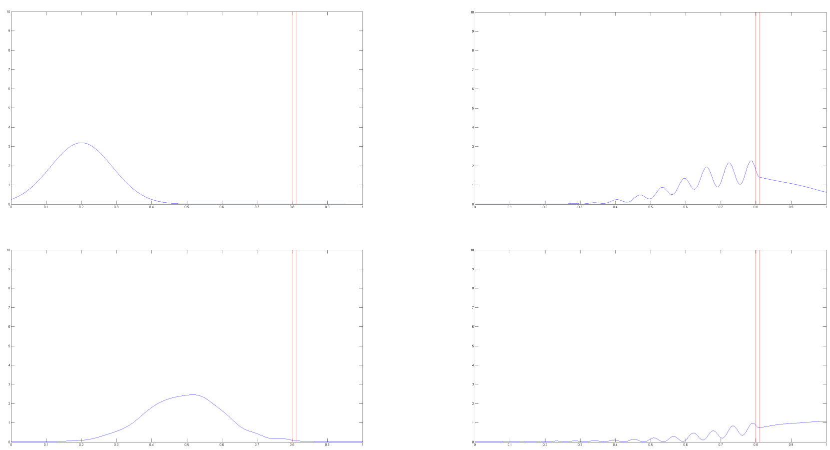

Figure 3.3: Barrier

3.2 2D Schrödinger Equation

The first example is a Gaussian wave in 2D

$$\psi(x, y) = \exp(ik_1 x + ik_2 y) \exp\left(-\frac{(x-0.5)^2 + (y-1)^2}{2\sigma^2}\right)$$

with $k_1 = -50$, $k_2 = 0$, $\sigma = 0.125$, $\Delta x = \dfrac{1}{25}$, $\Delta y = \dfrac{1}{25}$, $\Delta t = 2 \cdot 10^{-4}$ at $t = 0$, $30\Delta t$, $60\Delta t$, and $90\Delta t$. On a zero potential function, we know exact solution. In order to avoid non-physical reflection on y-direction, we set rectangle computation domain, which has a longer edge on y-direction. Fig 3.4

show this results. There is some unwilled reflection. I think it was occurred by inaccurate convolution coefficient, which should be updated in the future. So it is points to be duly considered at analysis results.

Next example is

$$\psi(x, y) = \exp(ik_1 x + ik_2 y) \exp\left(-\frac{(x-0.5)^2 + (y-1.5)^2}{2\sigma^2}\right)$$

with $k_1 = -50$, $k_2 = -50$, $\sigma = 0.125$, $\Delta x = \frac{1}{25}$, $\Delta y = \frac{1}{25}$, $\Delta t = 2 \cdot 10^{-4}$ at $t = 0,\ 30\Delta t,\ 60\Delta t$, and $90\Delta t$. This particle passes through y-axis with non-orthogonal incidence. Many boundary conditions cannot treat non-orthogonal incidence and cause non-physical wave figures. Our method show relatively reasonable results, although Fig 3.5 has some reflection by he same reason as Fig 3.4. This example indicates the angular independence of our transparent boundary conditions.

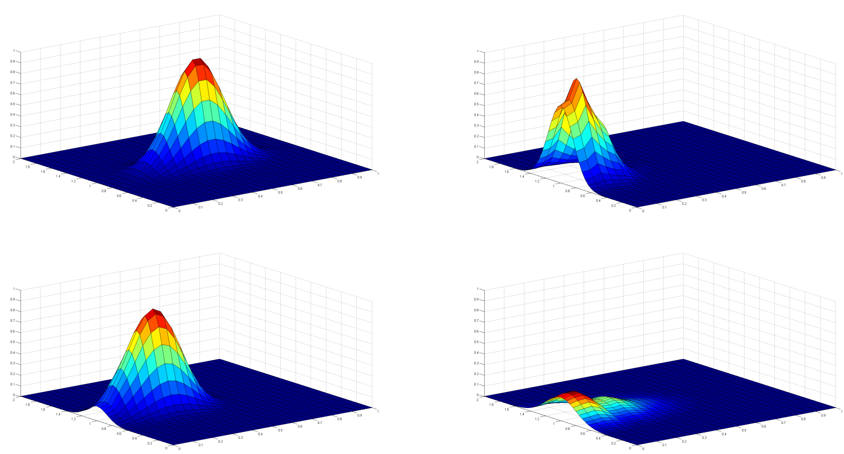

Figure 3.4: Orthogonal incidence free particle with velocity $k_1 = -50$, $k_2 = 0$, $\sigma = 0.125$, $\Delta x = \frac{1}{25}$, $\Delta y = \frac{1}{25}$, $\Delta t = 2 \cdot 10^{-4}$ at $t = 0,\ 30\Delta t,\ 60\Delta t$, and $90\Delta t$..

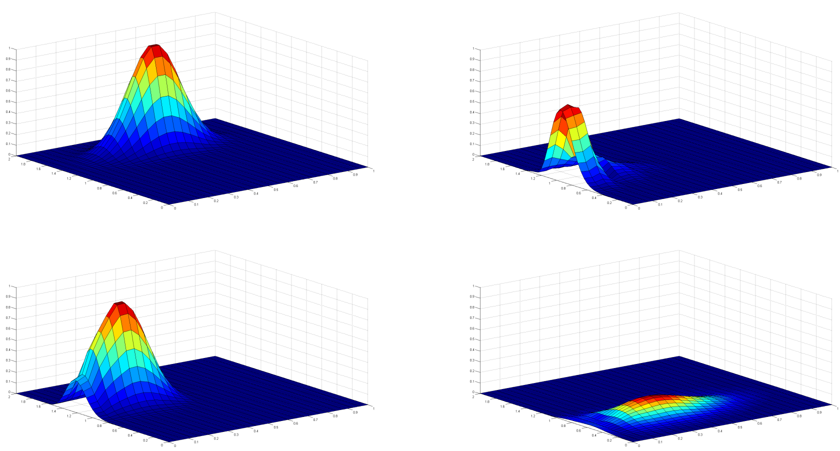

Figure 3.5: Non-orthogonal incidence free particle with velocity $k_1 = -50$, $k_2 = -50$, $\sigma = 0.125$, $\Delta x = \dfrac{1}{25}$, $\Delta y = \dfrac{1}{25}$, $\Delta t = 2 \cdot 10^{-4}$ at $t = 0,\ 30\Delta t,\ 60\Delta t,$ and $90\Delta t$

Chapter 4

Conclusion

We have looked around discrete transparent boundary conditions using Numerov method in 1D and 2D. Numerov extension induces high order scheme with cheap computing cost. The method had been made in MATLAB. Contained results show that it was effective numerical methods. It will contribute quantum wave simulation on a bound domain.

A reader may presume that we still do not treat whole rectangle boundary on 2 dimensional case, i.e., only one directional. In 1993, F. Collino derived corner conditions for wave equation on rectangle domain [5]. However, for the Schrödinger equation, no results are reported on this topic so far. It will be our next study.

Bibliography

[1] X. ANTOINE, A. ARNOLD, C. BESSE, M. EHRHARDT and A. SCHÄDLE, *A review of transparent and artificial boundary conditions techniques for linear and nonlinear Schrödinger equations, (2009).*

[2] X. ANTOINE and C. BESSE, *Unconditionally stable discretization schemes of non-reflecting boundary conditions for the one-dimensional Schrödinger equation, Journal of Computational Physics, 188 (2003), pp. 157-175.*

[3] X. ANTOINE, C. BESSE and V. MOUYSSET, *Numerical schemes for the simulation of the two-dimensional Schrödinger equation using non-reflecting boundary conditions, Mathematics of computation, 73 (2004), pp. 1779-1799.*

[4] A. ARNOLD, M. EHRHARDT and I. SOFRONOV, *Approximation, stability and fast calculation of non-local boundary conditions for the Schrödinger equation, Commun. Math. Sci, 1 (2003), pp. 501-556.*

[5] F. COLLINO, *High order absorbing boundary conditions for wave propagation models: straight line boundary and corner cases, Second International Conference on Mathematical and Numerical Aspects of Wave Propagation (Newark, DE, 1993), 1993, pp. 161-171.*

[6] M. EHRHARDT and A. ARNOLD, *Discrete transparent boundary conditions for the Schrödinger equation, Riv. Mat. Univ. Parma, 6 (2001), pp. 57-108.*,

[7] R. GORENFLO and F. MAINARDI, *Fractional calculus: integral and differential equations of fractional order, arXiv preprint arXiv:0805.3823 (2008).*

[8] Z. KALOGIRATOU, T. MONOVASILIS and T. SIMOS, *Numerical solution of the two-dimensional time independent Schrödinger equation with Numerov-type methods, Journal of mathematical chemistry, 37 (2005), pp. 271-279.*

[9] C. A. MOYER, *Numerov extension of transparent boundary conditions for the Schrödinger equation in one dimension, American Journal of Physics, 72 (2004), pp. 351-358.*

[10] M. SCHULTE and A. ARNOLD, *Discrete Transparent Boundary Conditions for the Schrdinger Equation–a Compact Higher Order Scheme, (2008).*

[11] J. C. STRIKWERDA, *Finite difference schemes and partial differential equations, Siam, 2004.*

국문초록

이 논문에서 우리는 누메로프 방법과 크랭크-니콜슨 방법을 이용해서 1차원과 2차원에 슈뢰딩거 방정식의 고차 알고리즘을 유도한다. 이런 과정에서 수치적 투과 경계 조건을 각 차원별로 유도한다. 마지막으로 1차원에서 유계 구간과 2차원에서 유계 직사각형 영역에서 이 조건을 실험한다.

주요어휘: 슈뢰딩거 방정식, 투과경계조건, 누메로프 방법
학번: 2012-20241